J Therm Anal Calorim (2012) 107:725–732
DOI 10.1007/s10973-011-1704-5

Kinetics study of thermal oxidative degradation of ABS containing flame retardant components

Jun Wang · Xu-fu Cai

Received: 24 January 2011 / Accepted: 26 May 2011 / Published online: 17 June 2011

Abstract The thermal oxidative degradation kinetics of pure acrylonitrile–butadiene–styrene (ABS) and the flame-retarded ABS materials with intumescent flame retardant (IFR) were investigated using Kissinger, Flynn–Wall–Ozawa, and Horowitz–Metzger methods. The results showed that the degradation of all samples included two stages, the activation energy at the first stage decreased by the incorporation of these flame retardant components, while increased at the second stage. The activation energy order of the flame-retarded ABS samples at stage 2 illustrates the relationship between the composition of IFRs and their flame retardancy, FR materials with appropriate acid agent/char former ratio has higher activation energy and better flame retardancy.

Keywords Intumescent flame retardant · Degradation kinetics · Activation energy · Thermal oxidative degradation

Introduction

Among non-halogenated flame retardants, intumescent flame retardant (IFR) is well known as a class of flame retardants in flammable polymers for some of their merits, such as low smoke, low toxicity, low corrosion, and no molten dropping during a fire [1, 2]. Generally, an IFR is composed of three active components: an acid source, such as ammonium polyphosphate (APP) that generates a mineral acid with temperature increase; a carbonization agent, which will react with the acid source to generate the char; and an acid agent which expands to form a swollen multicellular char by releasing nonflammable gas. There are many studies on the applications of the intumescent flame retardant. The IFRs generally include the following systems, i.e., ammonium polyphosphate + melamine + pentaerythritol [3–5], ammonium polyphosphate + triazine compound [6–8], marcromolecular char former contained system [9–11], mixture of melamine phosphate with pentaerythritol [12, 13] or their reaction product, single molecular IFR [2, 14], and so on.

From those contributions above mentioned, it is known that the flame retardancy of materials not only depends on their thermal stability but also on their degradation rate, char-forming rate and char yield [15, 16]. As a consequence, the thermal degradation details of the materials influence their flame retardancy to a considerable degree and deserve a deep investigation. Thermogravimetric (TG) analysis has been used widely to estimate the kinetic parameters of degradation processes, such as activation energies (E), reaction order (n), and the Arrhenius pre-exponential factor (A) [17–19], which can be calculated using various kinetic models such as Friedman, Kissinger, Coats-Redfern, Flynn–Wall–Ozawa, and Horowitz–Metzger methods. Kinetic data obtained from TG are very useful to help us understand the thermal degradation processes and mechanisms, and also may be used as input parameters for a model of thermal degradation reaction [20].

Our previous study has described the synthesis of a novel charring agent poly(p-propane terephthalamide) (PPTA) used for flame retardant acrylonitrile–butadiene–styrene (ABS) [21]. The incorporation of APP and PPTA into ABS can improve its thermal stability at high temperature and char yield during the degradation. In this

J. Wang · X. Cai (✉)
Department of Polymer Science and Engineering, Sichuan University, Chengdu 610065, China
e-mail: Caixf2004@sina.com

Table 1 LOIs and UL-94 rates of IFR-ABS systems

Sample	Components/mass%			LOI	UL-94
	ABS	APP	PPTA		
ABS-1	100	0	0	18.9	Fail
ABS-2	70	25	5	30.5	V-1
ABS-3	70	22.5	7.5	32.4	V-0
ABS-4	70	15	15	28.3	Fail

article, we studied the kinetics of the thermo-oxidative degradation of the flame-retarded ABS materials with IFR master batches with different acid agent/charring agent ratios using different kinetic models including Kissinger, Flynn–Wall–Ozawa, and Horowitz–Metzger methods.

Kinetic methods

In general, the degradation of solid polymer can be associated with the reactions, which may be represented by the process $A_{solid} \rightarrow B_{solid} + C_{gas}$, its reaction rate $d\alpha/dt$ can be written as

$$\frac{d\alpha}{dt} = kf(\alpha) \quad (1)$$

where $\alpha = (W_0 - W_t)/(W_0 - W_\infty)$ (W_0, W_t, and W_∞ are the initial, actual, and final mass of the sample, respectively, in the TG test), k is the degradation rate constant and the function $f(\alpha)$ depends on the specific degradation reaction mechanism.

The Arrhenius equation has the following formula:

$$k = A\exp\left(-\frac{E}{RT}\right) \quad (2)$$

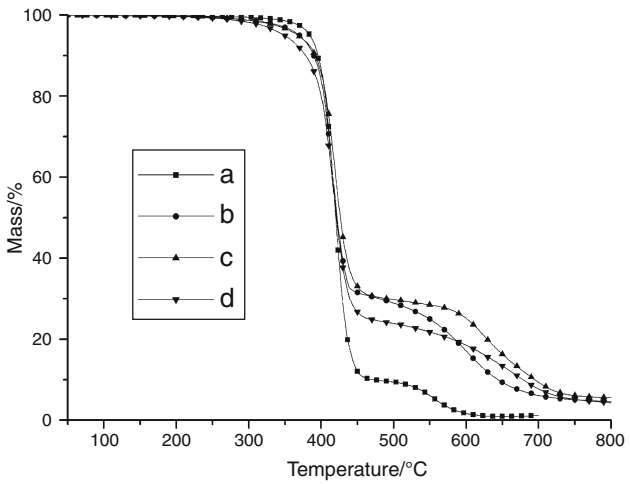

Fig. 1 TG curves of all samples at a constant heating rate of 10 °C min^{-1}

where A is the pre-exponential factor (s^{-1}), assumed to be independent of temperature, E is the activation energy (kJ mol^{-1}), T is the absolute temperature (K), and R is the gas constant (8.3136 J mol^{-1} K^{-1}).

A combination of Eqs. 1 and 2 leads to

$$\frac{d\alpha}{dt} = Af(\alpha)\exp\left(-\frac{E}{RT}\right) \quad (3)$$

If the sample temperature is changed by a controlled and constant heating rate β ($\beta = dT/dt$), Eq. 3 can be changed to

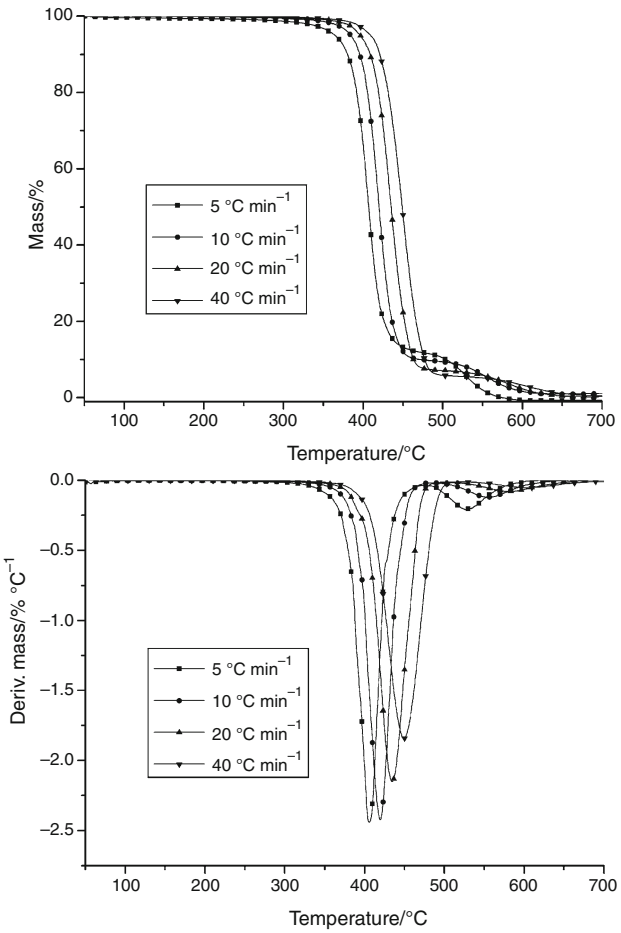

Fig. 2 TG and DTG curves of ABS-1 at different heating rates under air

$$\frac{d\alpha}{dT} = \frac{A}{\beta} f(\alpha) \exp\left(-\frac{E}{RT}\right) \quad (4)$$

Integration of the both sides of above equation and rearrangement give

$$g(\alpha) = \int_0^{\alpha} \frac{d\alpha}{f(\alpha)} = \frac{A}{\beta} \int_0^{T} \exp\left(-\frac{E}{RT}\right) dT \quad (5)$$

where g(α) is the integral function of conversion degree α. As far as the polymer is concerned, its degradation process, generally, obeys the sigmoidal or deceleration functions.

Based on the aforementioned equations, different kinetic methods such as Kissinger, Flynn–Wall–Ozawa, and Horowitz–Metzger methods were applied in this study.

Kissinger method (differential method)

Kissinger method involves the maximum temperatures (T_{max}) of the first derivative mass loss curves at multiple heating rates [22]. The activation energy can be determined by the Kissinger's method without a precise knowledge of the reaction mechanism, using the following equation:

$$\ln\left(\frac{\beta}{T_{max}^2}\right) = \left\{\ln\frac{AR}{E} + \ln\left[n(1-\alpha_{max})^{n-1}\right]\right\} - \frac{E}{RT_{max}} \quad (6)$$

where T_{max} is the temperature corresponding to the inflection point of the thermodegradation curves which corresponds to the maximum reaction rate, α_{max} is the conversion at T_{max}, and n is the reaction order. The activation energy E can be determined from a plot of $\ln(\beta/T_{max}^2)$.

Flynn–Wall–Ozawa and Horowitz–Metzger methods (integral methods)

Flynn–Wall–Ozawa method [23, 24], using the Doyle's approximation for the integration, has been expressed as:

$$\log\beta = -\frac{0.457E}{RT} + \left\{\log\left[\frac{AE}{g(\alpha)R}\right] - 2.315\right\} \quad (7)$$

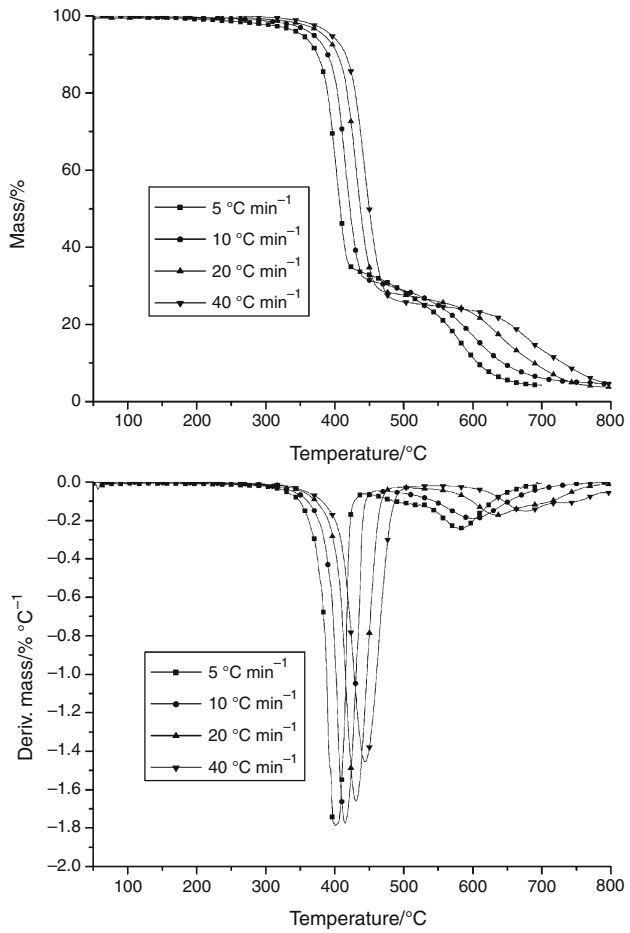

Fig. 3 TG and DTG curves of ABS-2 at different heating rates under air

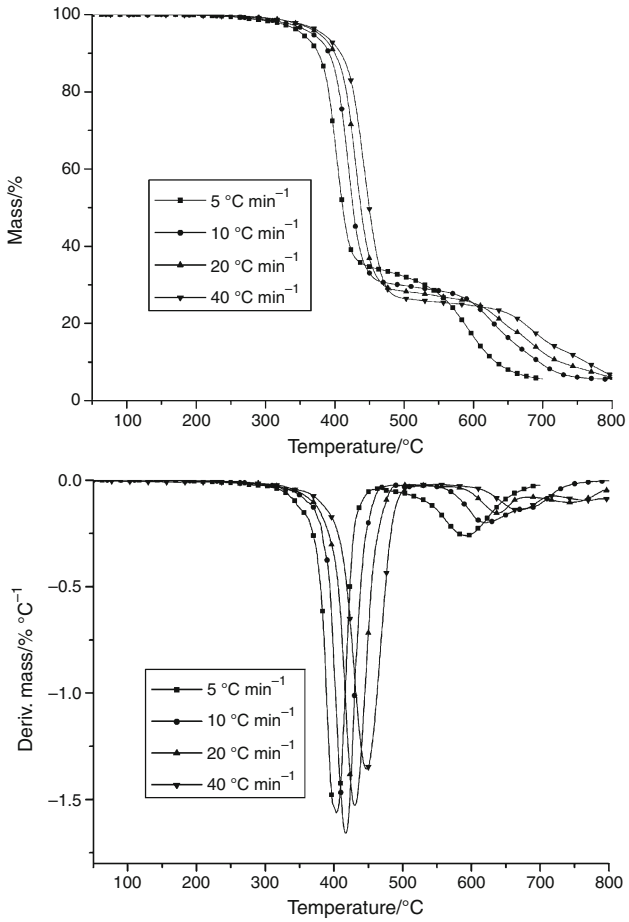

Fig. 4 TG and DTG curves of ABS-3 at different heating rates under air

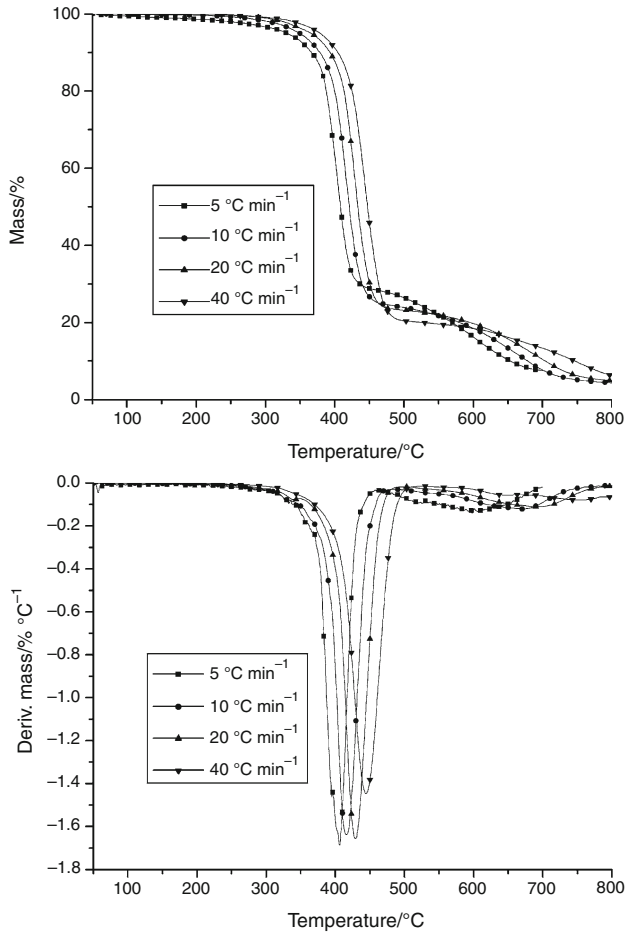

Fig. 5 TG and DTG curves of ABS-4 at different heating rates under air

Using Eq. 7, the linear representation of log β versus 1/T allows us to determine the activation energy with a given value of the conversion.

Horowitze–Metzger method [25] simplifies the exponential integral, obtaining the following equation:

$$\ln\left[\ln(1-\alpha)^{-1}\right] = \frac{E\theta}{RT_{\max}^2} \tag{8}$$

where θ is the difference between T and $T_{\max}$. The activation energy can be determined from a linear fit to the plot of ln[ln$(1-\alpha)^{-1}$] versus θ.

Experimental

Materials

The ABS copolymer (0215-A) was supplied by Jilin Petrochemical Co. (Jilin, China). Ammonium polyphosphate (APP) was obtained from Zhejiang Longyou GD Chemical Industry Corp. (Longyou, China). PPTA was synthesized and characterized in the previous article.

Flame-retarded samples preparation

The ABS resins with different acid agent/char former ratio, i.e., APP/PPTA ratio, were prepared via a twin screw extruder (TSSJ-25, Chengguang, China) at a temperature range of 200–230 °C. Then the extruded composites were injected into standard testing bars for test. The flame retardancy of IFR-ABS systems are listed in Table 1.

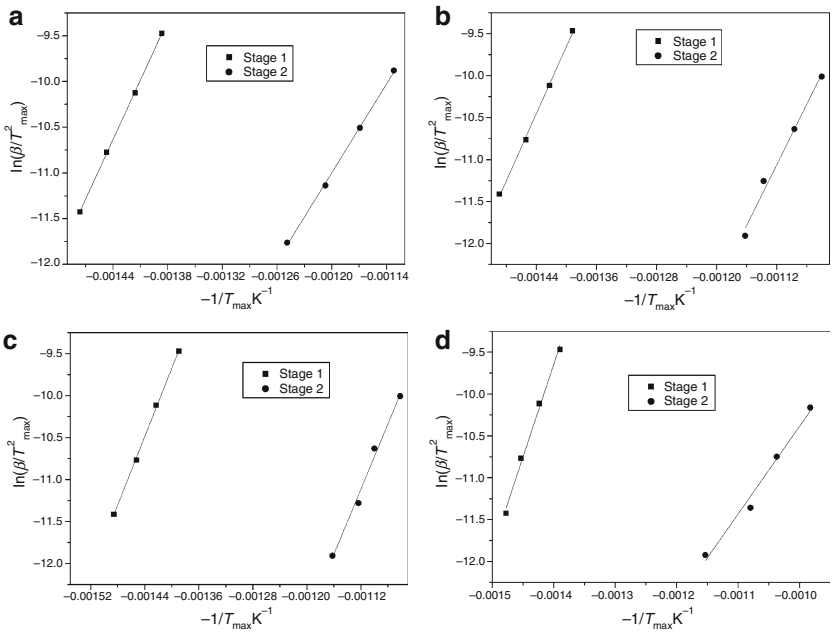

Fig. 6 Kissinger method applied to TG data at different heating rates under air: **a** ABS-1, **b** ABS-2, **c** ABS-3, and **d** ABS-4

Characterizations

LOI data of all samples were obtained at room temperature on an oxygen index instrument (XYC-75) produced by Chende Jinjian Analysis Instrument Factory, according to ASTM D2863-97 standard. The dimensions of all samples were 130 × 6.5 × 3 mm^3. Vertical burning rates of all samples were measured on a CZF-2 instrument produced by Jiangning Analysis Instrument Factory, with sample dimensions of 130 × 13 × 3 mm^3, according to ASTM D3801. The TG analysis was performed on a Mettler Toledo TG/DSC1 instrument thermal analyzer with a heating rate of 5, 10, 20, and 40 °C min^{-1} in the temperature range of 50–800 °C and a dynamic air flow of 60 mL min^{-1}. The amount of the sample used is 8–10 mg. Based on the original mass loss dependence of the temperature, the first derivative data, i.e., DTG were accordingly obtained.

Table 2 Activation energies of samples obtained by Kissinger and Horowitz–Metzger methods

Sample	Region	Activation energy by Kissinger method E/kJ mol^{-1}	Activation energy by Horowitz–Megzger method E/kJ mol^{-1}
ABS-1	Stage 1	180.12	258.15
	Stage 2	134.14	39.38
ABS-2	Stage 1	166.34	212.25
	Stage 2	149.93	41.86
ABS-3	Stage 1	169.35	197.25
	Stage 2	161.53	44.51
ABS-4	Stage 1	183.81	191.24
	Stage 2	87.1	32.21

Results and discussion

Figure 1 shows the TG curves of the flame-retarded ABS materials with IFRs having different acid agent/char former ratio (APP/PPTA ratio) at a constant heating rate of 10 °C min^{-1} under air atmosphere. It can be seen that pure ABS degrades through two steps, its initial degradation temperature is about 380 °C, and almost no char residue exists at over 600 °C. However, ABS containing APP/PPTA systems, ABS-1, ABS-2, and ABS-4, still have certain amount of char residues above 600 °C. This suggests the thermal stability of ABS has been enhanced by these components at high temperature. On the other hand, when the temperature is above 500 °C, the char residue of ABS-3 is much higher than ABS-2 and ABS-4. This is also in accordance with the results of LOI and UL-94 tests that the flame retardancy of ABS-3 is much better than ABS-2 and ABS-4.

For obtaining the kinetic information, such as the activation energy, the TG study has been conducted with the variation of the heating rates in this article. Figures 2, 3, 4, and 5 show the TG and DTG curves of the ABS containing different ratios of flame retardant components, corresponding to dynamic experiments carried out at different heating rates (5, 10, 20, and 40 °C min^{-1}).

Kinetics analysis using Kissinger method

Using the Kissinger Eq. 6, lines of $\ln(\beta/T_{max}^2)$ versus $-1/T_{max}$ for each stage of the thermal degradation were plotted for all samples. Figure 6 shows the representative plots for each stage of the thermal degradation of ABS-1, ABS-2,

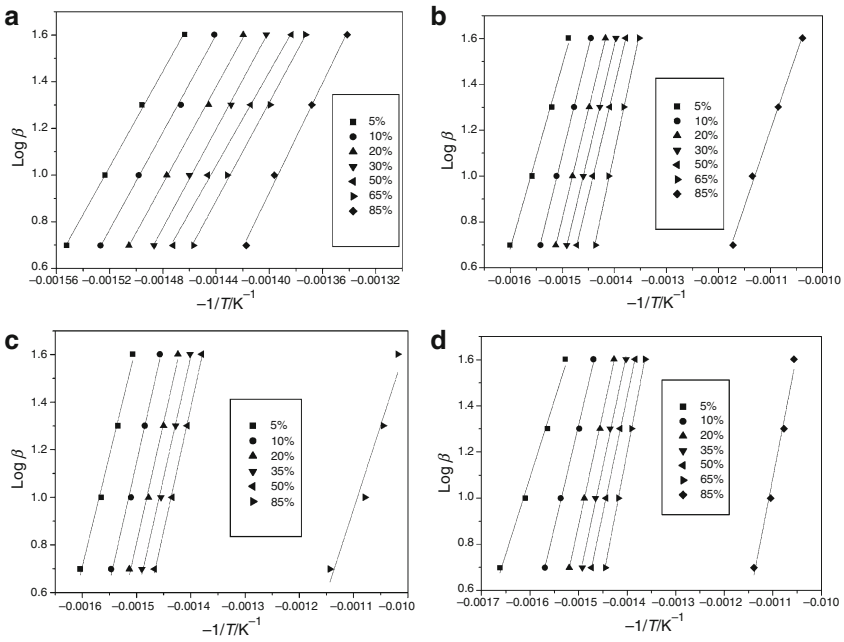

Fig. 7 Plots of log β versus $-1/T$ at various conversion values (α) in the range 5–85%: **a** ABS-1, **b** ABS-2, **c** ABS-3, **d** ABS-4

ABS-3, and ABS-4. The calculated degradation activation energies for every stage of all samples are listed in Table 2.

As can be seen, at the first stage, the degradation activation energy of ABS-1 is 180.12 kJ mol^{-1}. However, the activation energy of the flame-retarded ABS materials, ABS-2 and ABS-4, decreases to 166.34 and 169.35 kJ mol^{-1}, respectively, after addition of ABS-based IFR master batch with APP/PPTA molar ratios of 5.0 and 3.0. This is possibly due to the fact that the phosphoric acid species, as a degradation product of APP, attack the alkamide bonds of PPTA and leads to the formation of phosphoric ester and some cross-linking structures, which lower the degradation temperature of the system and decreases the activation energy. At the second stage, the activation energy of ABS-2 and ABS-4 reaches 149.93 and 161.53 kJ mol^{-1}, respectively, much higher than that of ABS-1. This is attributed to the yields of phosphorus residues formed in the first stage, which protect the substrate from heat and flame, thus make the materials more stable at higher temperature. In addition, at the second stage, the activation energy of the flame-retarded ABS with different acid agent/char former molar ratios decreases according to the following order: ABS-3 > ABS-2 > ABS-4, which is well coincided with their flame-retarding property order, i.e., ABS-3 > ABS-2 > ABS-4. This indicates that IFR-ABS with reasonable acid agent/char former has higher activation energy of thermal oxidative degradation, which is ascribed to the better stability of the charred layer with good quality formed in the burning process.

Kinetics analysis using Flynn–Wall–Ozawa method

Flynn–Wall–Ozawa model can also be used to calculate the activation energy of solid-phase reaction. According to

Table 3 Calculated activation energies at various conversions of the decomposition by Flynn–Wall–Ozawa method

Conversion	ABS-1		ABS-2		ABS-3		ABS-4	
	E/kJ mol^{-1}	r	E/kJ mol^{-1}	r	E/kJ mol^{-1}	r	E/kJ mol^{-1}	r
0.05	186.13	0.9995	152.91	0.9980	169.66	0.9968	121.28	0.9971
0.10	189.75	0.9992	168.45	0.9999	184.29	0.9967	161.82	0.9987
0.20	192.54	0.9994	171.74	0.9999	184.60	0.9974	176.81	0.9997
0.35	188.94	0.9994	173.74	0.9999	185.42	0.9976	182.45	0.9991
0.50	182.69	0.9991	174.02	0.9999	188.93	0.9989	184.06	0.9999
0.65	192.03	0.9990	194.36	0.9993	–	–	197.25	0.9999
0.85	213.53	0.9982	121.34	0.9983	128.29	0.9776	200.64	0.9936

r represents the correlation coefficient

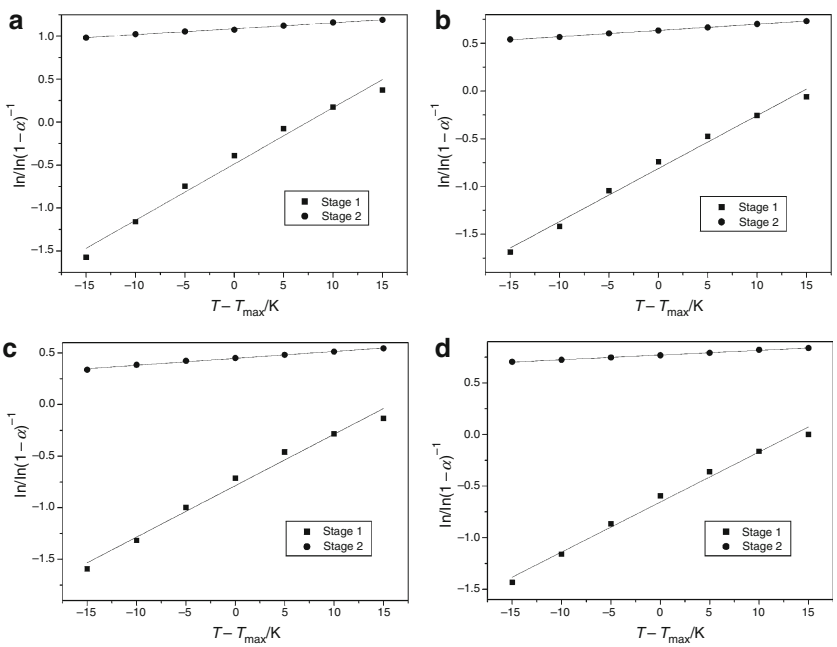

Fig. 8 Plots of $\ln[\ln(1-\alpha)^{-1}]$ versus θ for calculating the activation energies for all samples by Horowtiz–Metzger method

Eq. 7, at given value of the conversion, the activation energy can be obtained from a logarithmic plot of heating rates as a function of the reciprocal of temperature, since the slope of such a line is given by $-0.4567\ E/R$. For this study, the conversion values of 5, 10, 20, 35, 50, 65, and 85% were used. Figure 7 shows the fitting lines of ABS-1, ABS-2, ABS-3, and ABS-4 at the selected conversion values. All of the calculated activation energies are listed in Table 3. As can be seen, the activation energy of ABS-1 is much higher than ABS-2, ABS-3, and ABS-4 at the degradation ratios of 0.05–0.20. This implies that this stage of degradation does not result from the destruction of ABS. It is mainly from the degradation of APP and the reaction of APP and PPTA, after that, some cross-linking structures can be formed, which can act as a barrier to slow down the heat and mass transfer at high temperature. Therefore, the activation energies of ABS-2, ABS-3, and ABS-4 increase at elevated conversion. However, when the conversion is above 65%, the activation energies of ABS-1 and ABS-4 are higher than that of ABS-2 and ABS-3, which is not in accord with the results of Kissinger method. The possible reason can be related to the Doyle approximation made in the former, because the Doyle approximation has limitation of a range of 5–20%.

Kinetics analysis using Horowitz–Metzger method

In addition to the multiple heating rate method, Horowitz–Metzger method, as another integral method, was applied here to calculate the kinetic parameters. This method can determine the degradation activation energy using only one heating rate. In this study, the TG curves at a heating rate of 10° C $\min^{-1}$ were used to calculate the degradation kinetics for all samples. Using Eq. 8, the activation energy for each stage can be obtained from the linear fitting corresponding to the plot of $\ln[\ln(1-\alpha)^{-1}]$ versus θ, where θ is the difference between the referenced temperature (T_r) and the maximum temperature (T_{max}). This plot is shown in Fig. 8, with the chosen T_r from T_{max} -15 to $+15$ K in a step of 5 K and all the data are listed in Table 2. A comparison of these results with those previously obtained by Kissinger method shows that the activation energy at the first stage increases and the activation energy at the second stage shapely decreases. This may be attributed to the complicated degradation behaviors during these stages, which lead to the deviations in calculating activation energies via only one heating-rate TG method. However, a similar trend in the order of activation energies is also observed that the incorporation of APP and PPTA decreases the activation energy in stage 1 while increases in stage 2. Flame retardant components influence the degradation behaviors of ABS by self-degradation at relatively low temperatures, then forming a protective layer to increase the systems' thermostability.

Conclusions

The thermal oxidative degradation of pure ABS and flame-retarded ABS materials with different acid agent/char former ratios was analyzed using Kissinger, Flynn–Wall–Ozawa, and Horowitz–Metzger methods. The corresponding kinetic parameters were calculated to interpret the relationship between the composition of IFRs and the flame retardancy. The results showed the incorporation of APP and PPTA can lower the activation energies at early stages of the degradation while heighten them at later stages. The order of the activation energy of the various samples at the second stage is in good agreement with that of their flame retardancy, FR materials with appropriate acid agent/char former ratio has higher activation energy at stage 2, hence better flame retardancy.

Acknowledgements We would like to thank the generous financial support by the following grant: National Natural Sciences Foundation of China, Grant No. 50973066.

References

1. Horacek H, Pieh S. The importance of intumescent systems for fire protection of plastic materials. Polym Int. 2000;49:1106–14.
2. Gao M, Wu W, Yan Y. Thermal degradation and flame retardancy of epoxy resins containing intumescent flame retardant. J Therm Anal Calorim. 2009;95:605–8.
3. Demir H, Arkıs E, Balköse D, Ülkü S. Synergistic effect of natural zeolites on flame retardant additives. Polym Degrad Stab. 2005;89:478–83.
4. Anna P, Marosi Gy, Bourbigot S, Le Bras M, Delobel R. Intumescent flame retardant systems of modified rheology. Polym Degrad Stab. 2002;77:243–7.
5. Chiu S-H, Wang W-K. The dynamic flammability and toxicity of magnesium hydroxide filled intumescent fire retardant polypropylene. J Appl Polym Sci. 1998;67:989–95.
6. Li B, Xu MJ. Effect of a novel charring-foaming agent on flame retardancy and thermal degradation of intumescent flame retardant polypropylene. Polym Degrad Stab. 2006;91:1380–6.
7. CH Ke, Li J, Fang KY, Zhun QL, Yan Q, Wang YZ. Synergistic effect between a novel hyperbranched charring agent and ammonium polyphosphate on the flame retardant and anti-dripping properties of polylactide. Polym Degrad Stab. 2010;95:763–70.
8. Dai JF, Li B. Synthesis, thermal degradation, and flame retardance of novel triazine ring-containing macromolecules for intumescent flame retardant polypropylene. J Appl Polym Sci. 2010;116:2157–65.
9. Liu Y, Feng ZQ, Wang Q. The investigation of intumescent flame-retardant polypropylene using a new macromolecular charring agent polyamide 11. Polym Compos. 2010;30:221–5.
10. Almeras X, Dabrowski F, Bras ML, Delobel R, Bourbigot S, Marosi G, Anna P. Using polyamide 6 as charring agent in

intumescent polypropylene formulations. II. Thermal degradation. Polym Degrad Stab. 2002;77:315–23.
11. CX Lu, Chen T, Cai XF. Halogen-free intumescent flame retardant for ABS/PA6/SMA alloys. J Macromol Sci Phys. 2009;48:651–62.
12. Lv P, Wang ZZ, Hu KL, Fan WC. Flammability and thermal degradation of flame retarded polypropylene composites containing melamine phosphate and pentaerythritol derivatives. Polym Degrad Stab. 2005;90:523–34.
13. Balabanovich AI. Thermal degradation study of intumescent additives: Pentaerythritol phosphate and its blend with melamine phosphate. Thermochim Acta. 2005;435:188–96.
14. Halpern Y, Mott DM, Niswarder RH. Fire retardancy of thermoplastic materials by intumescence. Ind Eng Chem Prod Res Dev. 1984;23:233–8.
15. Chen YH, Liu Y, Wang Q, Yin H, Aelmans N, Kierkels R. Performance of intumescent flame retardant master batch synthesized through twin-screw reactively extruding technology: effect of component ratio. Polym Degrad Stab. 2003;81:215–24.
16. Chen Y, Wang Q. Thermal oxidative degradation kinetics of flame-retarded polypropylene with intumescent flame-retardant master batches in situ prepared in twin-screw extruder. Polym Degrad Stab. 2007;92:280–91.
17. Yang KK, Wang XL, Wang YZ, Wu B, Yin YD, Yang B. Kinetics of thermal degradation and thermal oxidative degradation of poly(*p*-dioxanone). Eur Polym J. 2003;39:1567–74.
18. Jin WP, Sea CO, Hac PL, Hee TK, Kyong OY. A kinetic analysis of thermal degradation of polymers using a dynamic method. Polym Degrad Stab. 2000;67:535–40.
19. Li LQ, Guan CX, Zhang AQ, Chen DH, Qing ZB. Thermal stabilities and thermal degradation kinetics of polyimides. Polym Degrad Stab. 2004;84:369–73.
20. Sun JT, Huang YD, Gong GF, Cao HL. Thermal degradation kinetics of poly(methylphenylsiloxane) containing methacryloyl groups. Polym Degrad Stab. 2006;91:339–46.
21. Jun W, Liu Y, Cai X. Effect of a novel charring agent on thermal degradation and flame retardancy of acrylonitrile–butadiene–styrene. J Therm Anal Calorim. 2011;103:767–72.
22. Kissinger HE. Reaction kinetics in differential thermal analysis. Anal Chem. 1957;29:1702–6.
23. Flynn JH, Wall LA. General treatment of the thermogravimetry of polymers. J Res Natl Bur Stand A Phys Chem. 1966;70A:487–9.
24. Ozawa T. A new method of analyzing thermogravimetric data. Bull Chem Soc Jpn. 1965;38:1881–6.
25. Horowitz HH, Metzger G. A new analysis of thermogravimetric data. Anal Chem. 1963;35:1464–7.